

CELLS IN SILICO (CIS) : A BIOMEDICAL SIMULATION FRAMEWORK BASED ON MARKOV RANDOM FIELD

KUNG-HAO LIANG

School of Biomedical Science, University of Nottingham, U.K.

E-mail: kunghaoliang@yahoo.com

This paper presents CIS, a biomedical simulation framework based on the markov random field (MRF). CIS is a discrete domain 2-D simulation framework emphasizing on the spatial interactions of biomedical entities. The probability model within the MRF framework facilitates the construction of more realistic models than deterministic differential equation approaches and cellular automata. The global phenomenon in CIS are dictated by the local conditional probabilities. In addition, multiscale MRF is potentially useful for the modelling of complex biomedical phenomenon in multiple spatial and time scales. The methodology and procedure of CIS for a biomedical simulation is presented using the scenario of tumor-induced hypoxia and angiogenesis as an example. The goal of this research is to unveil the complex appearances of biomedical phenomenon using mathematical models, thus enhancing our understanding on the secrets of life.

1. Introduction

Computational cell biology is an emerging discipline where biomedical simulations are employed for the study of cells and their microenvironments in various spatio-temporal scales.^{8,22} The E-cell²² and the Virtual Cell⁸ projects focus on the molecular and biochemical level within cells, addressing the dynamics of signal transductional, regulatory and metabolic networks. The sub-cell compartmental model are constructed and integrated gradually so as to simulate a particular facet (or pathway) of cells. The Epitheliome project is an example of tissue-level simulation, aiming to depict the epithelial cell growth and the social behavior of cells in culture.²⁵ Simulations on higher-level systems include Physiome,¹ and the modelling of many organs such as heart.¹⁵ Each scale of simulation shed light on different aspects of life.¹⁶

Biomedical simulations have been conducted in both the continuous and discrete domains. Differential equations are the key elements of continuous domain simulation,⁸ where the concentration of particular receptors, ligands, enzymes or metabolites are modelled at various spatial and temporal scales. This approach is limited by the fact that many biomedical phenomena are too complex to be described by sets of differential equations.¹¹ In addition, the deterministic differential equations are not adequate for describing many biological phenomenon with a stochastic nature. Alternatively, discrete domain simulation are processed on a spatio-temporal discrete lattice. The combination of Pott's model and Metropolis algorithm have been used to simulate cell sorting,¹⁰ morphogenesis,¹³ the behavior of malignant tumor²³ and the Tamoxifen treatment failure of cancer.²⁴

This paper presents cells in silico (CIS), a biomedical simulation framework based on markov random field (MRF). The local interactions between cells, various cytokines and the microenvironments dominates many biomedical phenomenon, including chemotaxis, the morphogenesis of neural systems, tumor angiogenesis and invasion. Thus, CIS is proposed with an emphasis on (i) the spatial modelling and visualization; (ii) the complex interactions between cells and microenvironments; (iii) non-deterministic (stochastic) modelling; and (iv) a general framework with solid mathematical foundation applicable to many biomedical applications.

MRF is a spatial stochastic framework in either the continuous or discrete domain.^{2,3} It has been applied to the modelling of protein-protein interaction networks⁷ and for solving various global optimization problems.^{9,14} MRF is closely related to the Pott's model, the Ising model in statistical mechanics, and cellular automata,¹¹ in the sense that all these models address the local interactions between spatially adjacent entities. The Ising model is in fact a sub-class of MRF (see Section 2). Compared with cellular automata, the stochastic nature of MRF enables the construction of more realistic biomedical models. In addition, MRF is extendable to a multiscale framework which facilitates the simulation of complex biomedical phenomenon on multiple degrees of details. Hence, it is adequate to serve as the basis of a biomedical simulation framework.

2. Markov Random Fields and CIS

Cells in Silico (CIS) is a discrete, stochastic framework for the modelling of cells, cytokines, extra cellular matrix and their spatial interactions. CIS employs a bottom-up approach. The biomedical phenomenon shown in CIS is not dictated by global deterministic equations, rather, it emerges when the local interactions of entities are computed iteratively, enabling the study of biological self-organization.

CIS is constructed upon a discrete domain MRF defined on a regular lattice of 2-D space. The lattice S represents a physical space of interest, such as the microenvironment of a tumor clump, or a certain type of tissue in culture, *in vitro* or *in vivo*. A random field $B \equiv \{B_i | 1 \leq i \leq n, i \in Z^+\}$ (Z denotes the integer) is a family of n discrete or continuous random variables defined on S . Each random variable B_i assumes a value c_m in the state space C_i , $C_i \in C \equiv \{C_i | 1 \leq i \leq n, i \in Z^+\}$. Each $B_i(s)$ represents the characteristic at a particular spatial location s , $s \in S$. It could be either a real biomedical characteristic (such as the neoplastic state of a cell, or the physical pressure induced by cell proliferation in a small space) or a hidden state which dictates a real characteristic as in a hidden Markov model. In this paper, a symbol in the upper case represents either a random field, a random variable or a set, while the lower case represents a particular realization of a random variable.

B is a MRF if and only of (i) all its realizations have positive probability, and (ii) the local conditional probability of its realizations manifest the Markov property:

$$\Pr(B(s) | B(S - s), s \in S) = \Pr(B(s) | B(s + q), s \in S, q \in Q) \quad (1)$$

where Q denotes the neighborhood.² For example, the second order neighborhood system

is

$$Q \equiv \{(x, y) \mid -1 \leq x, y \leq 1, x, y \in Z, (x, y) \neq (0, 0)\} \quad (2)$$

where a site s has 8 isotropic neighboring sites. The second order neighborhood system is adopted in this paper if not indicated specifically. The left-hand side of equation (1) shows that, in general, the state of a site is conditionally dependent on the state of all the sites except itself. The right-hand side indicates that it is only dependent on its neighbors. The equivalence of (1) forces the state of a site to be dictated by the local property in the neighborhood. Long range interactions of entities can still be achieved through the iteration of the local process.

The realization of $B_i(s)$ in a MRF follows a Gibbs distribution :

$$\Pr(B_i(s) = c_m) = \theta^{-1} * e^{-\frac{U_s(c_m)}{T}} \quad (3)$$

where T is the parameter of temperature which is generally set as 1, unless a simulated annealing strategy is adopted in the algorithm. U_s is the energy (*a.k.a.* cost) function associated with a particular realization of $B_i(s)$. U_s is determined by $B_i(s)$ and $B_i(s+q)$ according to the application. The definition of U_s determines the relative probabilities of a state, thus dictates the interaction of a site s and its neighboring sites. Different definitions of U_s results in different classes of MRF, such as the Gaussian MRF, the Ising model, the multi-level logistic model, etc. (cf. Li¹⁴ for a complete review). The normalization factor θ (*a.k.a.* partition function) is defined as

$$\theta^{-1} = \sum_{c_m \in C_i} e^{-\frac{U_s(c_m)}{T}} \quad (4)$$

This is to guarantee the sum of probabilities of all the possible realizations of $B_i(s)$ to be 1, i.e.

$$\sum_{c_m \in C_i} \Pr(B_i(s) = c_m) = 1 \quad (5)$$

A random variable $B_j(s)$ may be conditionally dependent on another random variable $B_i(s)$, depending on the application. The conditional probability has been modelled in many applications as a multivariate normal, which also follows a Gibbs distribution (cf. Li¹⁴ for proof):

$$\Pr(B_j(s) \mid B_i(s)) = \theta^{-1} * e^{-\frac{U_s(B_j(s) \mid B_i(s))}{T}} \quad (6)$$

In several occasions, the posterior probability $\Pr(B_i(s) \mid B_j(s))$ can be obtained using the Bayesian law, when the prior probability $\Pr(B_i(s))$, the probability of $B_j(s)$ and the likelihood probability $\Pr(B_j(s) \mid B_i(s))$ are all available:

$$\Pr(B_i(s) \mid B_j(s)) = \frac{\Pr(B_j(s) \mid B_i(s)) \Pr(B_i(s))}{\Pr(B_j(s))} \quad (7)$$

The prior probability $\Pr(B_i(s))$ reflects the prior knowledge (i.e. assumptions) about a particular random variable $B_i(s)$.

In CIS, all the probability models of equations (3), (6) and (7) can be used to represent various biomedical properties such as cell-cell or cell-matrix interactions. The probability model could be either homogeneous (i.e. consistent in the entire S) or regionally homogeneous (i.e. S comprise regions with different sets of probability models). We will show in the following applications how these probability models are constructed.

An important class of applications of MRF is for global optimization, where a state with minimal global energy $\sum U_s$ is pursued

$$\beta = \arg \min_{b \in B} \sum_{s \in S} U_s \quad (8)$$

The realization β is optimal with respect to either the maximum likelihood (ML)²⁷ or the maximum a posteriori (MAP)⁹ estimations using the probability model of (6) or (7) respectively. Due to the large solution space in all the non-trivial applications, β cannot be obtained analytically. An iterative state updating procedure is thus used, in either a deterministic or stochastic fashion. Deterministic methods update each site with the state which is associated to the largest probability. In contrast, stochastic relaxation methods (*a.k.a.* Markov Chain Monte Carlo methods) first randomly assigns a legitimate state for updating, computed the associate probability, then use a random number generator to determine whether the state updating action should take place under such a probability. The Gibbs distribution in (3) thus plays the role of the state transition Boltzmann probability in the simulated annealing algorithms (*a.k.a.* Metropolis algorithms), where T is gradually decreased, representing an annealing, stabilizing behavior of the system. The state updating procedure could proceed either with a random site visit or a raster scan. The simulated annealing algorithms are beneficial for searching the equilibrium states of the optimization problems.

CIS employs a stochastic relaxation strategy, which is advantageous for the modelling of a complex biomedical phenomenon. Since the aim of CIS is to study the dynamic, evolving behavior of life, T is defined as 1 in this paper, which is consistent with typical MRF approaches.¹⁴

3. Tumor, hypoxia and angiogenesis

A tumor is a clump of cancerous cells with distinct characteristics, such as the self-sufficiency in growth signals, capability of inducing angiogenesis, and metastasis.¹² The proliferation of tumor cells results in the lack of oxygen and nutrients in the center area of the tumor clump, inducing a high survival pressure and even necrosis. tumor cells are capable of secreting tumor angiogenic factors (TAFs) for attracting new capillaries from nearby blood vessels (i.e. angiogenesis). This capability of inducing angiogenesis is strengthened when the tumor cells are lack of oxygen (i.e. hypoxia).⁴⁵ Angiogenesis enables the tumor to obtain nutrients/oxygen and get rid of wastes via the circulatory system.⁶

Angiogenesis is an important characteristic of a malignant tumor, hence, the understanding of angiogenesis is very important for devising new methods for cancer prognosis and treatment. These new capillaries not only sustain the tumor growth but also provide

a gateway for metastasis. Known TAFs includes the vascular endothelial growth factor (VEGF), the basic and acidic fibroblast growth factors (FGF), scatter factors and many others. tumors have an increased expression of angiogenic factors, such as VEGF and FGFs, compared to their normal tissue counterparts.¹² In the mean time, the endogenous inhibitors such as thrombospondin-1 or β -interferon are down regulated.¹² At the beginning of angiogenesis, the subendothelial basement membrane of the nearby capillary vessels are degraded.²⁰ The endothelial cells are stimulated by the TAFs and grow toward the tumor clump, forming new capillary sprouts with the branching structure and anastomosis (i.e. loops).¹⁸ The anastomosis structure enables blood circulation. Finally, these endothelial cells synthesize a new basement membrane.²⁰

Research has shown that the hypoxia state of tumor cells can (i) stimulate the secretions of TAFs so as to invoke angiogenesis,^{19,5} and (ii) transform the cell to be more invasive.¹⁷ The reason of (ii) is because the hypoxia inducible factors (HIFs) within the cell detect the low oxygen levels, and therefore induce the high expression of c-Met protein, a receptor of hepatocyte growth factor (HGF, *a.k.a.* scatter factor-1). On binding the HGF expressed by the nearby stromal cells, c-Met triggers a signal transduction cascade which results in the increased cell motility, invasion and metastasis.¹⁷ This explains why an antiangiogenic treatment could risk to induce cancer cells to be prone to metastasis.¹⁷ The simulation on angiogenesis has been conducted using the combination of differential equations and the random walk method (e.g. Plank et al.¹⁸ and Stokes et al.²¹).

3.1. CIS Methodology

3.1.1. Define key entities as random variables.

The cell space S in this application is set as 256×256 sites to simulate an $1mm \times 1mm$ microenvironment of a tumor clump *in situ*. The tumor, the blood vessel (comprising both the endothelial cells and the basement membrane of the vessel) and tumor angiogenic factors (TAF) are identified as the key entities of a site, denoted as $T(s)$, $V(s)$ and $A(s)$ respectively. Hence, the random field $B \equiv \{T(s), V(s), A(s) | s \in S\}$ represents this microenvironment. The variable $T(s)$ has discrete states $\{T(s) | T(s) = 0, 1, 2, \dots\}$, where $T(s) = 0$ denotes the non-neoplastic state and $T(s) > 0$ denotes the degree of hypoxia in this neoplastic site, which is mainly caused by the excessive oxygen consumption caused by the neighboring proliferating tumor cells. The larger the number, the higher the degree of hypoxia. The variable $V(s) \equiv \{0, 1, 2\}$, where $V(s) = 0$ denotes no vessel in this site; $V(s) = 1$ denotes the vessel at s being capable of sprouting new branches; $V(s) = 2$ denotes the vessel being quiescent and not sprouting new branches. Those sites where both $V(s)$ and $T(s)$ are 0 represents either normal cells or extra cellular matrix. The variable $A(s)$, a positive real number, represents the concentration of all the angiogenesis factors in this current study, as has been used in many research (e.g., Plank et al.¹⁸). More elaborated simulation could be conducted where each angiogenesis factor is represented individually.

3.1.2. States initialization.

The tumor clump is a circle shown in light green in Figure 1(a). In these regions, $T(s) = 1$ and other regions $T(s) = 0$. The radius of this tumor clump is 14 pixels. Four vessels are in the nearby regions of this tumor clump. Each of these vessels is a circle with a radius of 7 pixels and shown in red in Figure 1(a). In these regions, $V(s)$ is randomly assigned as 1 or 2 at the probability of 10% and 90% respectively. The other regions $V(s) = 0$. The TAF concentration $A(s)$ is assumed to be 0 in the initial state. Note that each site is a geometrical location which is not necessarily a complete cell. Locating each single cell is not the main interest of this current simulation. An alternative way of initialization for a biomedical simulation is cell-based, where a template of cell is randomly placed in the tumor clump area. This could be achieved by the object-oriented programming technique. The cell-based simulation is exemplified by the Pott's model, where each generalized cell (an artificial unit which represents either real cells, extra cellular matrix or medium) are specified individually.¹³ In such a cell-based simulation, a more sophisticated set of random variables, such as the elaborated $T(s)$ and $A(s)$, should be introduced.

3.1.3. Define interactions between sites

The local conditional probability of the random variables defines the interactions between sites, which is very important for the modelling of biomedical properties. As is described in Section 2, the interactions are modelled using the local energy function U_s , which determines the conditional probability of a particular realization of the random field. Apart from MRF, the traditional approach utilizing differential (and difference) equations is very suitable for describing physical processes such as diffusion. A combination of both MRF and difference equations is therefore advantageous for CIS.

First, the tumor survival pressure $T(s)$ is modelled, which is an indication of hypoxia and pertains to the necrosis of tumor cells. The survival pressure and hypoxia are caused by the surrounding cells to the central area of the tumor clump, hence, $T(s)$ is determined using a multiscale neighborhood system, denoted as $Q_m(w)$:

$$Q_m(w) \equiv \{(x, y) | -w \leq x, y \leq w, w, x, y \in Z, (x, y) \neq (0, 0)\} \quad (9)$$

$Q_m(2)$, $Q_m(4)$, $Q_m(6)$ and $Q_m(8)$ are used so as to construct the gradient of survival pressure of the tumor clump. The interior area of the tumor clump suffer from more severe hypoxia. The probability of increasing the tumor survive pressure is defined as :

$$\Pr(T(s) \rightarrow T(s) + 1) = \prod_{q \in Q_m} [1 - \delta(T(s + q))][\delta(V(s + q))] \quad (10)$$

where δ is the Kronecker delta. The above equation specifies that the presence of tumor cells in a neighborhood increases the hypoxia. In addition, the presence of blood vessels in the neighborhood alleviates the condition of hypoxia.

Second, the flow of TAF concentration $A(s, t)$ is modelled. A tumor clump secretes TAF in a paracrine fashion, thus, a high concentration of TAF is assumed in the regions

adjacent to the tumor clump (i.e. $T(s) > 0$). The secreted TAF gradually diffuse through the space S , which is modelled using the diffusion equation, i.e.

$$\frac{\partial A(s, t)}{\partial t} = k \nabla^2 A(s, t) \quad (11)$$

where k is the diffusion parameter defined as 1.

Third, the directional growth of a blood vessel is modelled to be dictated by the concentration of TAF which exceed a threshold a_t . Define a thresholding function $\Lambda(x)$, which reports 0 if its variable $x \leq 0$.

$$\Lambda(x) = \frac{1}{2}[1 + \text{sgn}(x)](x) \quad (12)$$

Given a site s where $V(s) = 1$, the energy function $U(s + \eta)$, $\eta \in Q$ is defined as

$$U(s + \eta) = -\log\{\Lambda[A(s + \eta) - a_t]\} \quad (13)$$

Hence, the conditional probability

$$\Pr(V(s + \eta) = 1 | A(s), V(s)) = \frac{\Lambda[A(s + \eta) - a_t]}{\sum_{q \in Q} \Lambda[A(s + q) - a_t]} \delta(V(s) - 1) \quad (14)$$

Equation (12) specifies the probability of a site adjacent to a vessel being an extension of this vessel. The higher the TAF concentration $A(s + \eta)$, the higher the probability of vessel growth toward this direction. This is a simplified model. In reality, many other factors, such as the fibroblast cells and the extra cellular matrix in the connective tissue, also play important roles in determining the directional vessel growth.

3.1.4. Proceed Simulation.

A positive integer $\{t | t \in Z^+\}$ is used to represent the discrete time points. Every interaction model is associated to a particular time step τ . All the sites in S need to be updated when $t = \tau$. The states in the current time step depends on the state in the previous time step. CIS is programmed in the C++ object oriented style.

3.2. Results and Observations

Two simulations are conducted to manifest the angiogenesis and hypoxia occurred in the microenvironment of a tumor clump. The first simulation is a simple model where the hypoxia are not modelled. The initial states is shown in Figure 1(a) when $t = 0$. The time step is set as $\tau = 1$ for all the rules. The 2D visualization of the results when $t = 50, 200$ and 350 are shown in Figure 1(b)-(d), respectively. The TAF (depicted in blue) are diffused away from the tumor. The new capillary grows toward the tumor, forming a network with the branching and joining structure (i.e. anastomosis). The shape of these capillaries is visually similar to the results in Plank et al.¹⁸ which employs complex differential equations and a random walk approach. Note that the method in Plank et al.¹⁸ is more or less *ad hoc*, i.e. specific to a particular biomedical problem such as angiogenesis, while CIS is a general framework and paradigm which could be employed in many applications. Different

8

simulations using the identical parameter setting produce different yet similar pattern of capillary formation (data not shown). This is due to the stochastic nature of the algorithm.

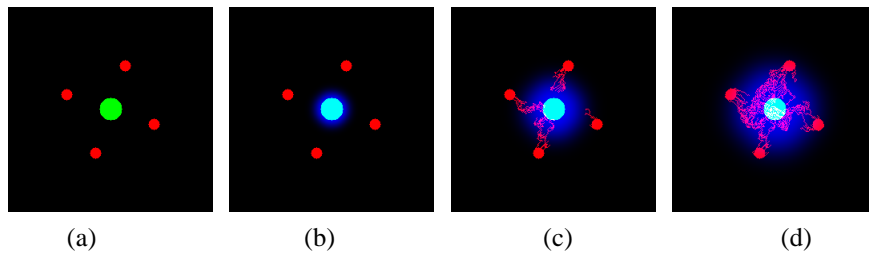


Figure 1. The 2-D visualization of CIS on tumor-induced angiogenesis (a) The initial condition of the simulation. The green region represents the tumor clump and the red regions represent the blood vessel. (b)-(d) CIS results when $t = 50, 200$ and 350 , respectively.

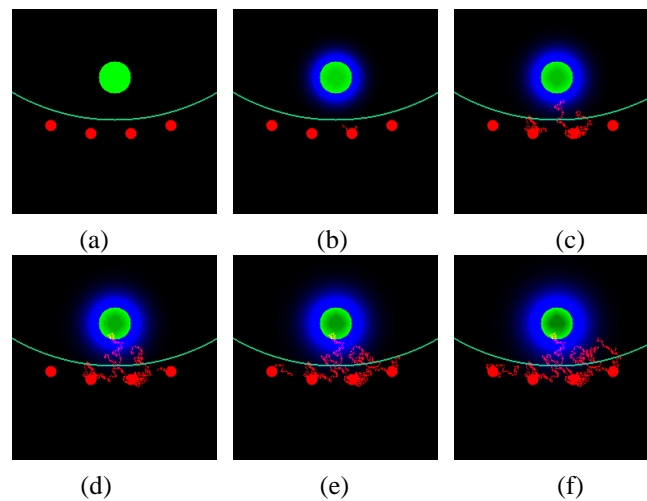


Figure 2. (a)-(f) The 2-D visualization of CIS of tumor-induced angiogenesis and hypoxia when $t = 0, 300, 450, 600, 750, 900$, respectively.

In the second simulation, the random field S simulates a cross sectional slice of the epithelium (top of Figure 2(a)) and connective tissue (bottom of Figure 2(a)) separated by the basal lamina (depicted in cyan). The tumor clump is situated in the epithelium, shown as a green circle with a radius of 20 pixels in Figure 2(a). Four blood vessels, shown as red circles with the same radius of 7 pixels, are situated in the connective tissue area. The interaction model of tumor hypoxia is employed. The time step is set as $\tau = 150$ for the hypoxia model, $\tau = 2$ for the angiogenesis, and $\tau = 1$ for all the other rules. The results when $t = 300, 450, 600, 750$ and 900 are shown in Figure 2(b)-(f), respectively. The value of $T(s)$ indicates the degree of hypoxia of a site. It shows that the color in the core are of the tumor clump turns from green to black, representing the gradual elevation of hypoxia.

A few new vessels begin to sprout on Figure 2(b). Several new vessels penetrate the tumor clump, preventing further necrosis on their adjacent sites on Figure 2(d)-(f).

4. Discussions and Conclusions

CIS, as well as all the other biomedical simulations, plays a complementary role to wet-lab experiments. It is evident that without solid biomedical knowledge acquired from wet-lab research and clinical observations, we cannot even start to identify the key entities for a simulation. An ideal simulation is conducted in concert with wet-lab experiments, starting with real data and finishing with real data. The biomedical models fill up the gaps of unknown knowledge between the two sets of real data. This gives rise to the systems biology, where a biomedical phenomenon is envisioned as a system of complicated interactions of many entities.

One of the plausible realizations of the above notion of systems biology is, for example, quantize a histopathology image of a cancerous tissue as the initial condition, replacing the procedure in section 3.1.2. The various parameter values, such as the time step τ , are also set according to the wet-lab measurements and observations. CIS are thus proceeded. The result of CIS are then compared with another set of microscopic image qualitatively or quantitatively.

CIS is extensible in terms of the complexity of simulation. The above example on tumor-induced hypoxia and angiogenesis can be elaborated by adding a variety of (i) entities, such as scatter factors, various cytokines, and the concentrations of oxygen and nutrient; (ii) interaction models, such as the tumor cell growth model on the presence of new blood vessels, and (iii) advanced data types such as the generalized cells.¹³

A further extension of CIS is toward multiscale simulation, addressing the complex, multi-level nature of biomedical phenomenon. The framework of Multiscale MRF has been well established (e.g. Wilson et al.²⁶). A multiscale simulation can illustrate both the between cell interactions and the within cell interactions under the same framework. For example, 2-D spatial grids of two different scales can be constructed, where each site in the first scale corresponds to $2^n \times 2^n$ (e.g. 4 or 16) sites in the second scale, as in a normal quad-tree structure. The first scale addresses the between cell interactions and the second scale addresses the within cell interactions. Activities in the two scales may take place in different paces, reflected as their distinct time steps τ . A multiple scale representation facilitates the incorporation of multiple levels of data, resulting a realistic model. The hypoxia model in Section 3 employs multiple neighborhood sizes, which is an example of multiscale realizations.

References

1. J.B. Bassingthwaite. The macro-ethics of genomics to health: The Physiome Project. *Comptes Rendus de l'Academie francaise*, 2002.
2. J.Besag. (1974). "Spatial interaction and the statistical analysis of lattice systems" (with discussions). *Journal of the Royal Statistical Society, Series B*, 36:192–236.
3. J.Besag. and Green, P. J. (1993). "Spatial statistics and Bayesian computation. *Journal of the Royal Statistical Society, Series B*, 55(1):25–37.

4. M. Blagosklonny. Antiangiogenic therapy and tumor progression. *Cancer Cell*, 5:13-17, 2004.
5. D.P. Bottaro and L.A. Liotta. Out of air is not out of action. *Nature*. 423:593-595, 2003.
6. W. B. Coleman and Gregory J. Tsongalis. The molecular basis of human cancer. Humana press Inc, 2002.
7. M. Deng, Z. Tu, F. Sun and T. Chen. Mapping gene ontology to proteins based on protein-protein interaction data. *Bioinformatics* 20:895-902, 2004.
8. C. Fall, E. Marland, J. Tyson, and J. Wagner. Computational cell biology, Springer-Verlag, 1st ed, 2002.
9. S. Geman and D. Geman, "Stochastic relaxation, Gibbs distributions, and the Bayesian restoration of images," *IEEE Trans. Patt. Anal. Machine Intell.*, vol. 6, pp. 721-741, 1984.
10. F. Graner and J.A. Glazier. Simulation of biological cell sorting using a two-dimensional extended Potts model. *Phys. Rev. Lett.* 86:4492-4495, 2001.
11. G.B. Ermentrout and L. Edelstein-Keshet. Cellular automata approaches to biological modelling. *J. theor. Biol.* 160 :97-133, 1993.
12. D. Hanahan and R.A. Weinberg. The hallmarks of cancer. *Cell* 100:57-70, 2000.
13. J.A. Izaquirre *et al.* CompuCell, a multi-model framework for simulation of morphogenesis. *Bioinformatics* 20:1129-1137, 2004.
14. S. Z. Li. Markov Random Field Modeling in Image Analysis. Springer-Verlag, 2001.
15. D. Noble. Modeling the Heart - from Genes to Cells to the Whole Organ. *Science* 295: 1678-1682, 2002.
16. D. Noble eds. In silico simulation of biological processes. Novartis Foundation Symposium, Wiley 2002.
17. S. Pennacchietti *et al.* Hypoxia promotes invasive growth by transcriptional activation of the met protooncogene. *Cancer Cell*. 3:347-361, 2003.
18. M. J. Plank and B. D. Sleeman. A reinforced random walk model of tumour angiogenesis and anti-angiogenic strategies. *Mathematical Medicine and Biology*. 20(2):135-181, 2003.
19. S. Roelwell and J.P.S. Knisely. Hypoxia and angiogenesis in experimental tumor models: therapeutic implications. in I.D. Goldberg and E.M. Rosen eds. Regulation of Angiogenesis, 1997.
20. E.M. Rosen and I.D. Goldberg. Regulation of angiogenesis by scatter factor. in I.D. Goldberg and E.M. Rosen eds. Regulation of Angiogenesis, 1997.
21. C.L. Stokes and D. A. Lauffenburger. Analysis of the roles of microvessel endothelial cell random motility and chemotaxis in angiogenesis. *J. theor. Biol.* 152: 377-403. 1991.
22. K. Takahashi *et al.* A multi-algorithm, multi-timescale method for cell simulation. *Bioinformatics* 20:538-546, 2004.
23. S. Turner and J. A. Sherratt. Intercellular Adhesion and Cancer Invasion: A Discrete Simulation Using the Extended Potts Model. *Journal of Theoretical Biology*, 216:85-100, 2002.
24. S. Turner, J. A. Sherratt and D. Cameron. Tamoxifen treatment failure in cancer and the nonlinear dynamics of TGF β . *Journal of Theoretical Biology*, vol. 229, pp. 101-111, 2004.
25. D.C. Walker *et al.* The epitheliome: agent-based modelling of the social behaviour of cells. Preprint, 2004.
26. R. Wilson and C. T. Li. A Class of Discrete Multiresolution Random Fields and its Application to Image Segmentation. *IEEE Trans. Trans. Patt. Anal. Machine Intell.* 25(1): 42-56, 2003.
27. J. Zhang. The mean field theory in EM procedures for markov random fields. *IEEE Trans. Trans. Sig. Process*, vol. 40, no. 10, pp. 2570-2583, 1992.